



HAL
open science

Cenozoic to Cretaceous paleomagnetic dataset from Egypt: New data, review and global analysis

Mireille M. Perrin, Ahmed Saleh

► **To cite this version:**

Mireille M. Perrin, Ahmed Saleh. Cenozoic to Cretaceous paleomagnetic dataset from Egypt: New data, review and global analysis. *Earth and Planetary Science Letters*, 2018, 488, pp.92-101. 10.1016/j.epsl.2018.02.014 . hal-02109229

HAL Id: hal-02109229

<https://hal.science/hal-02109229>

Submitted on 30 Apr 2019

HAL is a multi-disciplinary open access archive for the deposit and dissemination of scientific research documents, whether they are published or not. The documents may come from teaching and research institutions in France or abroad, or from public or private research centers.

L'archive ouverte pluridisciplinaire **HAL**, est destinée au dépôt et à la diffusion de documents scientifiques de niveau recherche, publiés ou non, émanant des établissements d'enseignement et de recherche français ou étrangers, des laboratoires publics ou privés.

1 **CENOZOIC TO CRETACEOUS PALEOMAGNETIC DATASET FROM EGYPT:**
2 **NEW DATA, REVIEW AND GLOBAL ANALYSIS**

3 Mireille Perrin¹ and Ahmed Saleh²

4 ¹ Aix-Marseille Univ, CNRS, IRD, Coll France, CEREGE, Aix en Provence, France.

5 ² National Research Institute of Astronomy and Geophysics, Egypt.

6 Corresponding author: perrin@cerege.fr ; +33 6 34 32 31 23

7 **Abstract**

8 Different phases of igneous activity took place in Egypt during the Mesozoic and the
9 Cenozoic and oriented samples were collected from three Cenozoic localities (Baharya oasis
10 in the Western Desert, Abu Had in the Eastern Desert and Quseir along the Red Sea coast),
11 and four Cretaceous localities (Toshki & Abu Simbel south of Aswan, and Shalaten & Abu
12 Shihat along the Red Sea coast). Rock magnetic properties of the samples indicate magnetite
13 and titanomagnetite as the main carrier of the remanent magnetization. Following stepwise
14 demagnetization, characteristic remanent directions were identified only for 62% of the
15 samples, a fairly low rate for that type of samples, and 8 new paleomagnetic poles were
16 calculated. All our Cenozoic poles fall clearly off Master Polar Wander Paths proposed for South
17 Africa. Therefore, all paleomagnetic results, previously published for Egypt, were compiled
18 from Cretaceous to Quaternary. The published poles largely overlap, blurring the Egyptian
19 Apparent Polar Wander Path. A new analysis at the site level was then carried out. Only poles
20 having a kappa larger than 50 were selected, and new pole positions were calculated by area
21 and by epoch, when at least 3 sites were available. Even though the selection drastically
22 reduced the number of considered poles, it allows definition of a reliable Cenozoic apparent
23 polar wander trend for Egypt that differs from the South African Master Polar Wander Path
24 by about 10-15°. If the Cretaceous igneous poles are in good agreement with the rest of the
25 African data, the sedimentary poles plot close to the Cenozoic portion of the South African

26 Master Polar Wander Path, a discrepancy that could be related either to inclination flattening
27 and/or error on age and/or remagnetization in the Cenozoic.

28

29 **Key words:** *Paleomagnetism, Cenozoic, Cretaceous, Egypt*

30 **1. Introduction**

31 During the Phanerozoic, Egypt was affected by intermittent igneous activity, mainly in
32 relation with the Late Precambrian fracture system. A compilation of more than 150 isotopic
33 ages (Rb/Sr with a few K/Ar) was used to construct a sequence of Phanerozoic igneous
34 activity in Egypt (Meneisy, 1990): i) Early Paleozoic vulcanicity associated with or closely
35 related to the Pan-African tectono-thermal event; ii) Late Paleozoic magmatism related to the
36 initial break-up of Pangea and the closure of the Tethys; iii) Mesozoic igneous activity related
37 to the rifting of the South Atlantic, the corresponding Africa-South America compression and
38 Afro-Arabian strike slip faulting; iv) Cenozoic volcanic pulses associated with the Red Sea
39 opening; and v) Quaternary igneous activity, not very well documented, that could be of early
40 Pleistocene age along the Red Sea and in the south Western Desert.

41 It is often difficult to decipher between the different episodes and, in the absence of
42 radiometric dating, paleomagnetism is a very convenient tool to estimate the age of an
43 intrusion or an extrusion. Paleomagnetic data can further constrain the local and global
44 tectonic activity in the area. Although there have been many paleomagnetic studies
45 undertaken in the past century, the definition of an apparent polar wander path is not
46 straightforward for Egypt and new Cretaceous and Cenozoic samples were collected in order
47 to improve the quantity and quality of paleomagnetic information from this region. All
48 samples were drilled in the field using a gasoline-powered drill and oriented using both
49 magnetic and sun compasses.

50 **2. Cretaceous igneous activity and sampling**

51 Mesozoic igneous activity resulted in the intrusion and/or extrusion of various types of
52 rock, abundant and diversified in size, form and composition. The basaltic rocks and alkaline
53 ring complexes can generally be related to two main phases of igneous activity: i) a *Late*
54 *Jurassic-Early Cretaceous phase* (140±15 Ma) and ii) a *Late Cretaceous-Early Tertiary*
55 *phase* (90±20 Ma). Most of the Mesozoic igneous activity is located in the southern Eastern
56 and Western Deserts and in Sinai (Meneisy, 1990).

57 Most samples related to the *Late Jurassic-Early Cretaceous* phase are alkaline ring
58 complexes from the south Eastern Desert. This 140 Ma episode of alkaline magmatism in
59 Egypt coincided with a major episode of alkaline magmatism occurring in the areas
60 surrounding the South Atlantic and related to the initial rifting of Africa from South America.
61 Ring complexes of the same age have also been reported in northeastern Sudan. Examining
62 the tectonic distribution map of the ring complexes in the south Eastern Desert, it can be noted
63 that these complexes are confined to a slightly curved zone of weakness that extends 200 km
64 and trends in a NE direction parallel to the Aswan trend, the regional fault system of Wadi
65 Halfa, Aswan, and Marsa Alam. The generation of this magma may have been triggered by
66 some "hot spot" mechanism.

67 The *Late Cretaceous-Early Tertiary phase* is perhaps one of the most documented
68 events of alkalic igneous activity in Egypt, formed during large scale strike-slip faulting in
69 Afro-Arabia. The best record of the event is undoubtedly the volcanic rocks of Wadi Natash,
70 about 125 km ENE of Aswan, along the boundary between the Nubian sandstone and the
71 Precambrian basement complex, for which a mantle-plume source has been suggested
72 (Mohamed, 2001). In the south Western Desert, some alkaline volcanics that pierce Paleozoic
73 sandstones can be correlated to the Wadi Natash volcanics (Oweinat and Gilf El Kebir areas).

74 The same alkaline magmatism gave rise to Gebel El Kahfa, Gebel Abu Khrug, and partly
75 Gebel El Naga and Gebel Mansouri ring complexes.

76 Different localities, supposed to be Cretaceous in age, were sampled south of Aswan
77 and along the Red sea (Figure 1): 3 sites (29 samples) in Toshki area [22.78°N, 31.48°E] and
78 3 sites (26 samples) north of Abu Simbel city [22.43°N, 31.21°E], in the south Western
79 Desert; 21 dikes (122 samples) in the wadi Abu Shihat, along the Red Sea; and 4 flows (25
80 samples) close from Shalaten (23.12°N, 35.46°E). As isotopic ages are missing, the age of the
81 basaltic rocks was based on field relations, within wide error limits, and therefore has to be
82 taken with caution.

83 **3. Cenozoic igneous rocks and sampling**

84 Several volcanic events took place during the Cenozoic, the earliest of Paleocene age
85 being the continuation of the extensive late Cretaceous igneous activity. Mid Tertiary
86 volcanism is widespread, with several pulses in the Late Eocene (Red Sea doming and
87 extension) followed by phases related to the opening of the Red Sea and Gulf of Suez and
88 ranging in age from Late Oligocene to Middle Miocene (Meneisy, 1990). This volcanism is
89 uniformly basaltic and widely distributed in the northern part of Egypt and in Sinai. Basaltic
90 extrusives cover a large area beneath the Nile delta and adjacent parts of the Western Desert.
91 Isolated outcrops also occur along the Fayum-Rawash, and Cairo-Suez stretches. In the south
92 Western Desert, some Tertiary basaltic occurrences are sparsely distributed, associated
93 sometimes with minor occurrences of acid to alkaline rocks. Along the Red Sea coast, south
94 of Quseir, some dolerite flows occur. A few scattered basaltic dykes and plugs intruding
95 Nubian sandstones in the south Eastern Desert are also considered of Tertiary age. Finally in
96 Sinai, several Tertiary basaltic outcrops occur, especially in the western and central areas.

97 The Tertiary basaltic rocks are found mainly in the form of sheets, dikes, sills, widening
98 sometimes into plugs, cinder cones or small ridges. The basalts of Abu Zabel, Abu Rawash,
99 Djebel Qatrani, and the Cairo-Suez district are described as quartz tholeiitic basalt whereas
100 the basalts from Baharya Oasis and the Nile district are alkali olivine basalts. Trace elements
101 abundances and Sr-Nd-Pb-Hf isotopic signatures are consistent with contributions from two
102 distinct source regions, one similar to the Afar plume and the other analogous to the
103 rejuvenated Pan-African lithosphere that likely underlies most of the continent (Endress et al,
104 2011).

105 Using K/Ar on whole rock ages, Meneisy (1990) proposed different volcanic episodes:
106 i) *Late Eocene-Early Oligocene (40±10 Ma)* possibly due to emergence related to a
107 shallowing of the Tethys, and volcanics developing along the fracture systems associated to
108 these tectonically-controlled movements, in the south Western Desert (Gebels Oweinat,
109 Arkenu, Kamil, Darb El Arbain); ii) *Oligo-Miocene phase (24±2 Ma)* related to the opening
110 of the Red Sea - the Red Sea formed by continental rifting in the Late Oligocene or Early
111 Miocene and widened through a combination of normal faulting and of dike injection - well
112 documented in northern Egypt (in the north Western Desert at Wadi Samalut and Gebel
113 Qatrani, in Cairo-Suez area, mainly at Abu Zabel, and along the Red Sea, south of Qusier)
114 and in western Sinai (Gebels Matulla and Araba); and iii) *Lower-Middle Miocene phases (20,*
115 *18 and 15 Ma)* as in Baharya Oasis.

116 More recently, $^{40}\text{Ar}/^{39}\text{Ar}$ dating confirms the short duration of the Oligo-Miocene phase
117 in the Cairo-Suez area, with ages indistinguishable from those of early syn-rift Red Sea-
118 parallel dikes in western Arabia, Sinai and the Eastern Desert of Egypt. This suggests that the
119 Red Sea propagated through Arabia/Sudan as a single, very rapid pulse and only stopped at
120 the interface with stronger Neotethyan oceanic crust near the coast of the modern
121 Mediterranean Sea. Although the volcanism of northern Egypt is volumetrically smaller than

122 that of Afar, it has been proposed (Bosworth et al, 2015) that it played a similar role as a
123 trigger for a large-scale rift event, with a Cairo mini-plume. The age of the igneous activity of
124 the Baharya Oasis was found to be similar to the rest of the Oligo-Miocene phase ($^{40}\text{Ar}/^{39}\text{Ar}$
125 ages between 21-25 Ma, Bosworth et al, 2015), questioning the existence of the last volcanic
126 phase of Meneisy (1990).

127 During previous field work, different localities have been already sampled in the Oligo-
128 Miocene phase (Perrin et al, 2009): 2 flows (27 samples) at Abu Zabel (30.28°N, 31.36°E)
129 north of Cairo; 3 flows (23 samples) around Quatrani (29.71°N, 30.65°E) in the Fayum
130 district; and 3 sites (18 samples) in Wadi Nukhul (29.02°N, 33.16°E), western Sinai. All these
131 basalts yielded $^{40}\text{Ar}/^{39}\text{Ar}$ age around 23 Ma (Kappelman et al, 1992; Bosworth et al, 2015).
132 New sampling was carried out in three other localities: 3 sites (13 samples) in the Baharya
133 Oasis area (28.36°N, 28.88°E); 4 flows (28 samples) in Wadi Abu El Had (28.03°N,
134 32.35°E), north Eastern Desert; and 5 dikes (35 samples) close from Quseir (25.75°N,
135 34.39°E), along the Red Sea.

136 **4. Temperature dependence magnetic susceptibility**

137 Temperature dependence magnetic susceptibility is a quick and sensitive method for the
138 identification of magnetic phases and for the determination of titanomagnetite composition
139 (Lattard et al 2006). Furthermore, the degree of reversibility of the heating and cooling runs
140 allows an estimate of phase changes, which can be interpreted in terms of stability of the
141 original magnetic phases (Vahle et al., 2007). Low-field thermomagnetic measurements (K-T
142 curves) under controlled atmosphere were carried out on selected samples for all sites using a
143 CS-3 apparatus coupled to a KLY-3 bridge (AGICO, Czech Republic). Samples were
144 progressively heated from room temperature (RT) up to 600°C and subsequently cooled back

145 to RT. For most samples, low-temperature susceptibility (from about -195°C to RT) was also
146 recorded using a CS3-L apparatus coupled to the KLY-3 bridge.

147 The five associations, seen in our samples, are illustrated by representative K-T curves
148 (Figure 2):

- 149 a) One-fourth of our samples display a single magnetic carrier with a high Curie point
150 (T_c around $550-575^{\circ}\text{C}$) and a good reversibility between the heating and cooling
151 curves. This is typical of the presence of almost pure magnetite (Ti-poor magnetite). If
152 this behavior was seen in some Cenozoic samples of Abu Zabel, here it is only found
153 in the Cretaceous basalts of Abu Shihat and Shalaten;
- 154 b) Besides the Ti-poor magnetite, another carrier of magnetization is also present in one-
155 third of the samples. The lower T_c ($350-400^{\circ}\text{C}$) and the significant irreversibility
156 between heating and cooling curves point to titanomaghemite that get transformed at
157 higher temperature. This association is present in Cenozoic (Qatrani and Baharya
158 flows), and Cretaceous (Abu Shihat dykes and Shalaten flows) sites.
- 159 c) Samples from Abu Had are even more complex, with three magnetic phases: i) Ti-rich
160 magnetite with low T_c ($100-150^{\circ}\text{C}$) and reversible curves; ii) Ti-maghemite with
161 intermediate T_c ($390-420^{\circ}\text{C}$) and a significant irreversibility; and iii) Ti-poor
162 magnetite with high T_c ($500-550^{\circ}\text{C}$).
- 163 d) Another third of our samples contain a mixture of Ti-rich magnetite and the Ti-
164 maghemite. If the irreversibility of the curves is taken as a qualitative measure of the
165 degree of maghemitization, most of our samples display relatively small degrees of
166 maghemitization, a characteristic feature of the basaltic rocks. This behavior is present
167 in Cenozoic and Cretaceous sites (Baharya, Toshki, Abu Simbel, Shalaten).

168 e) Finally, some samples from the south Western Desert (Toshki and Abu Simbel) carry
169 mostly the Ti-rich magnetite phase with T_c below 200°C and no other phases at higher
170 temperatures.

171 **5. Paleomagnetic analysis**

172 One specimen from each core was stepwise demagnetized using alternating fields (AF),
173 up to a maximum of 170mT with an automated degauss system coupled with a 2G
174 Superconducting Rock Magnetometer, or thermal demagnetization up to 600°C with an
175 homemade oven. Characteristic Remanent Magnetizations (ChRM) were calculated using
176 principal component analysis with Maximum Angular Deviation (MAD) always below 4, and
177 their means estimated by Fisher's statistic (α_{95} and kappa). It is worse being reminded that, if
178 kappa is independent of the number of sites N and always reflects the dispersion of a
179 population around the mean, α_{95} is meaningless for very small population and will not be
180 given in the tables for $N < 5$. Demagnetization diagrams were done with the PuffinPlot
181 software (Lurcock and Wilson, 2012), and the analysis with the help of the PmagPy software
182 (Tauxe et al, 2016). Considering the latitudes of our sites, the inclination of the present dipole
183 field (PDF) can be estimated between 47° for the northern sites (Baharya, Abu Had) and 40°
184 for the southernmost sites (Toshki, Simble, Shalaten).

185 All samples from **Qusier** plugs are characterized by an intensity of their Natural
186 Remanent Magnetization (NRM) a thousand times lower than all other samples, a very large
187 dispersion of their NRM directions, and completely erratic AF demagnetizations that do not
188 isolate a ChRM. Very likely sulfurs related to some phase(s) of metamorphism are the
189 magnetic carriers in these samples that will not be considered any further.

190 After removal of a viscous component in the present field, all **Baharya oasis (BH)**
191 basalts present a reverse ChRM with unblocking fields ranging from 10-30mT to 25-60mT

192 (e.g. Figure 3a). At the end of the demagnetizations, spurious component of magnetizations
193 can be acquired, maybe related to transformation of Ti-maghemite at high temperature or
194 through gyromagnetic remanence or a higher sensitivity to anhysteretic remanent
195 magnetization at the end of AF demagnetization. Dispersion at the site level is fairly high but
196 without relation to the sites (Figure 4a). However, the specimen mean value is within 1° of the
197 site mean (Table 1) and was favoured considering the small number of sites.

198 The magnetic behaviour of the **Toshki (TK)** basalt is the most simple found in this
199 study, with mostly one component of magnetization (e.g. Figure 3b), carried by Ti-rich
200 magnetite. The ChRMs calculated from TK1 and TK3 seem statistically different from those
201 of TK2 (Figure 4e) but both site and specimen means are still within one degree.

202 After removal of a secondary component that is either viscous or a partial IRM
203 overprint, the ChRM carried by most samples of **Abu Simble (AS)** is easy to define (e.g.
204 figure 3a). However, the ChRM directions are very dispersed, as well at the site level than at
205 the locality (Figure 4f), especially in inclination. This dispersion cannot be explained by
206 analytical uncertainties, but is more likely related to an orientation problem with samples not
207 really in place that was difficult to see with the outcrops buried in the desert sand. The
208 hypothesis is supported by the close agreement between the Toshki and the Abu Simbel mean
209 results, apart only by 3.5° .

210 During AF demagnetization, all basalts sampled in wadi **Abu Had (AH)**, from **Abu**
211 **Shihat (SH)** dykes and **Shalaten (ST)** basalt present two components of magnetization as
212 illustrated by Figure 3c. The low coercivity components are more or less pronounced, but
213 always removed in fields between 5-15mT and almost randomly distributed. This points to an
214 isothermal process for the acquisition of these secondary components, likely during lightning
215 strikes. However, at higher fields or temperatures, reverse ChRMs can be isolated from most
216 of the samples. The dispersion is fairly large for Abu Had (Figure 4d), likely because of

217 imprecisions on the definition of the final components that can represent sometime less than
218 1% of the NRM (e.g. close-up of the end of the orthogonal diagram on figure 3c). However,
219 the reliability of the mean value is supported by the agreement here also within 1° between
220 specimen mean and site mean (Table 1). Shalaten samples give a reverse ChRM fairly well
221 grouped at the site level (Figure 4h) and significantly different from the recent field. Abu
222 Shihat site means cluster around the present dipole field position (Figure 4g).

223 Mean ChRM directions are presented by site (Figure 5a) and by area (Figures 5b), and
224 the corresponding Virtual Geomagnetic Pole (VGP) positions (Table 1) are compared with
225 two Master Polar Wander Paths (MPWP) for South Africa (BC2002: Besse and Courtillot,
226 2002; T2008: Torsvik et al, 2008; Figure 5c).

227 Even though the two MPWPs are fully comparable for the period 0-130Ma of interest
228 for our study, all our Cenozoic pole positions are clearly off the paths. The Cretaceous poles
229 from Toshki TK, Abu Simbel AS and Shalaten ST1 are in good agreement with the MPWP
230 but not the poles from Shalaten ST2 and Abu Shihat SH and SH10. If the reliability of poles
231 ST, AS, and SH can be questioned (only one site or $kappa < 50$), all other poles are robust.

232 **6. Comparison with previously published data**

233 In order to better understand this discrepancy, all Cenozoic and Cretaceous
234 paleomagnetic data published for Egypt were searched. 41 references published between
235 1973 and 2016 were found but full text could be retrieved only for 33 of the references. In
236 some cases, the same data was published in different papers and only the most recent one was
237 considered. Altogether, 57 poles from 27 papers were compiled (33 Cenozoic poles and 24
238 Cretaceous poles, Table 2, Figure 6a). After a mild selection ($kappa > 50$), the 50 remaining
239 poles (29 Cenozoic poles and 21 Cretaceous poles, Figure 6b) present a significant dispersion
240 but mainly a fairly large overlap between the Cenozoic and Cretaceous poles with no obvious

241 correlation between VGPs and ages. Different reasons can be evoked to explain that
242 distribution. The first one is obviously related to dating uncertainties and unfortunately not
243 much can be done besides getting new, reliable radiochronologic ages. Another important
244 reason is clearly related to remagnetization and possible estimates of intermediate components
245 of magnetization, as shown with our data. Finally there is a real problem of data averaging,
246 with some areas that have been extensively sampled. In order to check the influence of these
247 last two factors, a compilation was made at the site level for all data with ages ranging from
248 Miocene to Cretaceous.

249 **7. Compilation of the Cenozoic data at the site level**

250 Site means could be retrieved from all papers except three references (El Shazly and
251 Krs, 1973; Lofty, 1998; Kent and Dupuis, 2003) that will therefore not be included in the
252 following analysis. Altogether, 247 sites (145 igneous and 102 sediments, Table 3) are
253 available for the period 14-59 Ma, mainly in the northern part of Egypt (Figure 1) but with a
254 fairly good temporal distribution, except maybe for the Paleocene (5 poles per Ma in average;
255 Figure 7a). However, when all site means are considered, the dispersion is extremely large
256 (Figure 7b).

257 A large part of that dispersion is related to the Shalaten data. Niazzi and Mostafa
258 (2002) proposed 4 distinct populations (G1 to G4) for their Shalaten data: the G1 group
259 supposed to be compatible with their geological and geochronological data, that would
260 confirm the Early Miocene age around 20 Ma; the other groups being structurally affected by
261 the Red Sea opening. However, looking at the almost random dispersion of the site mean
262 directions, with usually pretty tight site distributions (Figure 7c), and our own results on the
263 same area of the Red Sea coast (Figures 3c and 4g), the hypothesis of a remagnetization of
264 these isolated hilly masses by lightning strikes is more likely.

265 Removing the 39 igneous sites from Shalaten (Niazzi and Mostafa, 2002), as well as our
266 two Shalaten sites and all site means with $k \leq 50$, the dispersion of the remaining 134 sites
267 (64 sedimentary, 70 igneous) is drastically reduced (Figure 7d). However the overlapping of
268 the remaining site poles is still large, with a slight difference between results obtained from
269 igneous and sedimentary rocks. Different types of averaging of the whole dataset have been
270 tempted (e.g. 5 or 10 Ma window) but none can clarify the APWP likely because of age
271 uncertainties, but also because all intermediate components were not removed by selecting
272 $k > 50$ and maybe from an over-representation of certain areas.

273 In order to test the influence of the over-representation of certain areas, a new analysis
274 was carried out with all sites, including our new sites, having a kappa larger than 50. When in
275 a given area, and for a given period, at least 3 poles were available, a new mean VGP was
276 calculated (Table 4, Figure 7e). In locations where many different studies have been published
277 (Baharya, Cairo and Qatrani, Table 2), the new analysis drastically reduced the number of
278 means but really improves the definition of the proposed poles (Table 4). Cairo and Qatrani
279 areas are very good example of what we called 'over-representation' of data: 10 and 9 poles
280 were respectively published (Table 2), and only 2 and 3 poles are now proposed (Table 4). In
281 areas where only one publication per locality was available (Minia, Qatara and Mokatam), it
282 basically confirms the published determinations, with a slight improvement related to the
283 rejection of sites with $k \leq 50$. Finally for some areas (Oweinat, Tereifiya, and Gilf Kebir), no
284 VGPs could be estimated.

285 The four recalculated sedimentary poles (Table 4) describe a coherent evolution toward
286 the present field even though the relation between poles and ages remains unclear. This can be
287 explained by the averaging at a given site of sediments of slightly different ages (sections).
288 Averaging the site poles for individual sedimentary units, with a roughly 10Ma age windows,
289 give a better definition of the mean poles for the different epochs of the Cenozoic:

- 290 • Lower Miocene (12-23Ma), 9 sites, 202°E, 77°N, $A_{95}=1.6$, $K=983$
- 291 • Oligocene (23-34Ma), 9 sites, 157°E, 76°N, $A_{95}=6.1$, $K=71$
- 292 • Upper Eocene (34-40Ma) 20 sites, 159°E, 72°N, $A_{95}=4.3$, $K=59$
- 293 • Lower Eocene (40-53Ma), 26 sites, 159°E, 69°N, $A_{95}=4.1$, $K=49$

294 The corresponding apparent polar wander path (APWP) for Egypt is highlighted in
 295 Figure 7e by a dashed arrow. Despite a discrepancy between the lower Miocene poles, the
 296 Oligocene and Eocene new igneous poles (Table 4, Figure 7e) are in good agreement with the
 297 sedimentary data, comforting the reliability of the proposed path, and its clear difference from
 298 the BC2002 MPWP (Figure 7e). An anticlockwise rotation on the order of 10-15° is necessary
 299 to bring back the Egyptian curve onto the South African MPWP. The Cenozoic collision of
 300 continental Africa and Eurasia during the closure of the Neo-Tethys Ocean altered the
 301 kinematic and tectonic evolution of the Africa plate, including a slowdown in Africa's
 302 northward motion relative to its surrounding plates (DeMets and Merkouriev, 2016) and an
 303 accompanying fragmentation of the plate into distinct Arabia, Nubia and Somalia plates.
 304 However, fragmentation of the African plate seems to have begun at 29–24 Ma, when
 305 incipient rifting along the present Gulf of Aden and Red Sea signalled the break-off of the
 306 Arabian peninsula from Africa (Bosworth and Stockli, 2016). Therefore the observed
 307 difference between the Egyptian and South African polar wander path seem difficult to be
 308 explain solely by the opening of the Red Sea, except if the fragmentation started in the
 309 Eocene. However, a similar anticlockwise rotation of 11° has been observed (Ibrahim, 1999)
 310 from paleomagnetic poles of the Afar area.

311 **8. Compilation of the Cretaceous data at the site level**

312 Site means could be retrieved from all papers except for one reference (El Shazly and
 313 Krs, 1973) that will therefore not be included in the following analysis. Altogether, 224 sites

314 (118 igneous and 106 sediments, Table 3 and Figure 8a) are available for the Cretaceous
315 (around 3 data/Ma), mainly in the southern part of Egypt (Figure 1). Using the same selection
316 criteria than for the Cenozoic ($kappa > 50$), the number of poles is roughly cut by half but the
317 dispersion of the remaining 103 sites (72 igneous, 31 sedimentary, Figure 8b) is significantly
318 reduced. When the igneous site poles have a fairly isotropic distribution, there is a clear trend
319 in the sedimentary results.

320 As for the Cenozoic, all site results have been reanalysed by areas and by period. Only
321 four igneous and four sedimentary poles (Table 4, Figure 8c) pass the selection criteria (at
322 least 3 sites and $K > 50$). All igneous Cretaceous poles are in good agreement with the 78-98
323 Ma portions of the Besse and Courtillot (2002) MPWP for South Africa (BC2002),
324 underlying a Late Cretaceous age for all this volcanic activity (Late Cretaceous-Early Tertiary
325 phase). Sedimentary poles fall close from the Cenozoic portion of BC2002. Considering the
326 trend seen in the distribution of the site determinations (Figure 8b), an inclination problem
327 could be suspected. The elongation/inclination E/I method (Tauxe et al, 2008) was used to try
328 to recognize a possible inclination flattening. The distribution is considered *pathological* by
329 the method. This likely means that the scatter is not either of geomagnetic in origin or from
330 sedimentary flattening. Another possible explanation would be either an error in age or a
331 remagnetization of the sediments in the Cenozoic. New radiometric and paleomagnetic data
332 are needed to decide between these hypotheses.

333 **9. Conclusion**

334 43 sites (278 specimens), sampled in Cenozoic and Cretaceous horizons all over Egypt,
335 have been paleomagnetically studied. The analysis has been hampered by the very common
336 occurrence of secondary components acquired by isothermal process, likely during lightning
337 strikes, especially along the Red Sea coast. New mean paleomagnetic directions have been

338 obtained from 26 individual sites, and 8 new mean poles proposed (2 Cenozoic and 6
339 Cretaceous) and compared with the Master Polar Wander Paths proposed for South Africa.
340 The Cretaceous poles from Toshki, Abu Simbel and Shalaten ST1 are in good agreement with
341 the MPWPs but not the Cretaceous poles from Shalaten ST2 and Abu Shihat, and all our
342 Cenozoic pole positions.

343 A compilation of all Cenozoic and Cretaceous paleomagnetic data published for Egypt
344 (41 references published between 1973 and 2016) did not help to understand the discrepancy.
345 After a mild selection ($kappa > 50$), the 50 remaining poles (29 Cenozoic poles and 21
346 Cretaceous poles) present a significant dispersion but mainly a fairly large overlap between
347 the Cenozoic and Cretaceous poles with no obvious correlation between VGPs and ages.

348 In order to check the influence of some of the reasons that could explain that overlap, a
349 compilation was made at the site level for all data with ages ranging from Middle Miocene to
350 Cretaceous. Beside rejection of all results clearly influenced by IRMs, choosing to limit the
351 dispersion at the site level to $kappa > 50$ reduced the occurrence of intermediate components of
352 magnetization. Finally to avoid the over-representation of certain areas, new mean poles have
353 been calculated taking into account all sites available in a given area, for a given period.

354 The four recalculated sedimentary poles for the Cenozoic describe a coherent evolution
355 toward the present field even though the relation between poles and ages still remains unclear.
356 Averaging the site poles for individual sedimentary levels, with a ~10Ma age windows, give a
357 better definition of the mean poles for the different epochs of the Cenozoic, and allow to
358 propose a new Cenozoic apparent polar wander path for Egypt. The seven new igneous poles
359 fit fairly well the sedimentary data, confirming the reliability of the proposed path. An
360 anticlockwise rotation on the order of 10-15° is necessary to bring back the Egyptian curve
361 onto the South African MPWP, similar to what have been described by Ibrahim (1999) for the
362 Afar rift.

363 The four igneous recalculated poles for the Cretaceous are in good agreement with the
364 78-98 Ma portion of the BC2002's MPWP for South Africa, underlying an upper Cretaceous
365 age for all this volcanic activity. The four sedimentary poles fall close from the Cenozoic
366 portion of BC2002's MPWP, a discrepancy that could be related to inclination flattening
367 and/or error on age and/or remagnetization in the Cenozoic. New radiometric and
368 paleomagnetic data are needed to decide between these hypotheses.

369 **Acknowledgement**

370 This work was supported through a contribution CNRS-INSU, 2-year PHC IMHOTEP
371 project 20734YC, 2-month postdoctoral fellowship for A.S. from the French MAEE, and the
372 support of NRIAG for fieldwork and travel to France for A.S. The authors wish to
373 acknowledge Pierre Camps's help in the Montpellier laboratory, and to thanks Lisa Tauxe for
374 her very helpful review.

375

376

377

378

379 **References**

- 380 Abd El-All E.M., 2004. Paleomagnetism and rock magnetism of El-Naga ring complex, South
381 Eastern Desert, Egypt. *NRIAG J. Geoph.*, 3, 17-31.
- 382 Abdeldayem, A.L., 1999. Palaeomagnetism of some Cenozoic sediments, Cairo-Fayum area,
383 Egypt. *Phys. Earth Planet. Inter.*, 110, 71-82.
- 384 Abdeldayem, A.L., 1996. Paleomagnetism of some Miocene rocks, Qattara depression,
385 western desert, Egypt. *J. Afr. Earth Sci.*, 22, 525-533.
- 386 Besse, J., Courtillot, V., 2002. Apparent and true polar wander and the geometry of the
387 geomagnetic field over the last 200 Myr. *J. Geophys. Res.*, 107, doi:10.1029
388 /2000JB000050.
- 389 Bosworth, W., Stockli, D.F., Helgeson, D.E., 2015. Integrated outcrop, 3D seismic, and
390 geochronologic interpretation of Red Sea dike-related deformation in the Western
391 Desert, Egypt – The role of the 23 Ma Cairo “mini-plume”. *J. Afr. Earth Sci.*, 109,
392 107–119.
- 393 Bosworth, W., Stockli, D.F., 2016. Early magmatism in the greater Red Sea rift: timing and
394 significance. *Can. J. Earth Sci.*, 53, 1158–1176, dx.doi.org/10.1139/cjes-2016-0019.
- 395 DeMets, C., Merkouriev, S., 2016. High-resolution estimates of Nubia–Somalia plate motion
396 since 20 Ma from reconstructions of the Southwest Indian Ridge, Red Sea and Gulf of
397 Aden. *Geophys. J. Int.*, 207, 317–332.
- 398 El Shazly, E.M., Krs, M., 1973. Paleogeography and paleomagnetism of the Nubian
399 Sandstone, Eastern Desert of Egypt, *Geol. Rundschau*, 62, 212-225.
- 400 El-Shayeb H., El-Hemaly I.A., Abdel Aal E., Saleh A., Khashaba A., Odah H., Mostafa R.,
401 2013. Magnetization of three Nubia Sandstone formations from Central Western Desert
402 of Egypt. *NRIAG Journal of Astronomy and Geophysics*, 2, 1, 77-87. ISSN 2090-9977,
403 <https://doi.org/10.1016/j.nrjag.2013.06.011>.

404 Endress C., Furman T., Abu El-Rus M.A., Hanan B.B., 2011. Geochemistry of 24 Ma basalts
405 from NE Egypt: source components and fractionation history. In *The Formation and*
406 *Evolution of Africa: A Synopsis of 3.8 Ga of Earth History*. Van Hinsbergen, D. J. J.,
407 Buitter, S. J. H., Torsvik, T. H., Gaina, C. and Webb, S. J. (eds). Geological Society,
408 London, Special Publications, 357, 265–283. DOI: 10.1144/SP357.14 0305-
409 8719/11/\$15.00

410 Hussain A.G., Aziz Y., 1983. Paleomagnetism of Mesozoic and Tertiary rocks from East El
411 Owenat area, southwest Egypt, *J. Geophys. Res.*, 88, 3523-3529.

412 Hussain A.G., Soffel H., Schult A., 1980. Paleomagnetism of the Quatrani basalts, western
413 desert. *Egypt, Acad Sc. Res. Tech.*, 224, 1-9.

414 Hussain A.G., Schult A., Soffel H., 1979. Palaeomagnetism of the basalts of Wadi Abu
415 Tereifiya, Mandisha and dioritic dykes of Wadi Abu Shihat, Egypt. *Geophys. J. Royal*
416 *Astronomic. Soc.*, 56, 55-61.

417 Hussain A.G., 1977. Magnetization of some sedimentary rocks units in Bahariya area,
418 western desert, Egypt. *Helwan Obs Bull*, 141, 1-2.

419 Hussain A.G., Schult A., Soffel H. and Fahim M., 1976a . Magnetization and paleomagnetism
420 of Abu Zaabal and Abu Rawash basalts (Egypt). *Bull. Helwan Inst Astro Geo*, 134, 1-
421 15.

422 Hussain A.G., Schult A., Soffel H., Fahim M., 1976b. Magnetization of the Nubian sandstone
423 of Aswan area, Idfu-Mersa Alam and Qena-Safaga districts, Egypt, *Bul Helwan Inst.*
424 *Astro Geo.*, 133, 1-14.

425 Ibrahim, E.H., 1999. Paleomagnetism and the Afro-Arabian rift system. *Egyptian J. Geol.*, 42,
426 257-272.

- 427 Kappelman J., Simons, E.L., and Swisher III C.C., 1992. New Age Determinations for the
428 Eocene-Oligocene Boundary Sediments in the Fayum Depression, Northern Egypt. The
429 Journal of Geology, 100, 647- 6681.
- 430 Kent D.V., Dupuis C., 2003, Paleomagnetic study of the Paleocene-Eocene Tarawan chalk
431 and Esna shale: dual polarity remagnetizations of Cenozoic sediments in the Nile Valley
432 (Egypt). MicroPal., 49, 139-146.
- 433 Lattard D., Engelmann R., Kontny A. and Sauerzapf U., 2006. Curie temperatures of synthetic
434 titanomagnetites in the Fe-Ti-O system. Reassessment of some methodological and
435 crystal chemical effects. J. Geophys. Res., 111, B12S28.
- 436 Lofty H.I., Odah H.H., 2015. Paleo-tectonic positions of Northeast Africa during Cretaceous–
437 Paleocene: Paleomagnetic study on East Gilf Kebir Plateau basalts [59Ma],
438 Southwestern Desert, Egypt, NRIAG J. Geophys., 4, 32-43.
- 439 Lofty H.I., 2011. Active concomitant counterclockwise rotation and northwards translation of
440 Africa during the Albian-Campanian time: a paleomagnetic study on the Wadi Natash
441 alkaline province (104-78 Ma), southeastern desert, Egypt, Palaeogeography,
442 Palaeoclimatology, Palaeoecology, 310, 176-190.
- 443 Lofty H.I., Van der Voo R., 2007. Tropical northeast Africa in the middle-late Eocene:
444 Paleomagnetism of the marine-mammals sites and basalts in the Fayum province,
445 Egypt. J. Afr. Earth Sc., 47, 135-152.
- 446 Lofty H.I., Abd El-All E., 2003. Paleomagnetic study on the middle Eocene limestone, the
447 Tertiary basalt and the iron mineralization, west El Minia, Egypt. Annals Geol Surv
448 Egypt, 26, 507-528.
- 449 Lofty H.I., Odah H.H., 1998. Paleomagnetic differentiation of two Tertiary basaltic episodes
450 in northern Egypt during the Late Eocene and early Miocene, in northeast Egypt: Hint

451 of petrochemical and petrologic diversity, Bull. Fac. Sci Geology, Assiut Univ., 27,
452 301-320.

453 Lofty H.I., Van der Voo R., Hall M., Kamel O.A., Abdel Aal A.Y., 1995. Paleomagnetism of
454 Early Miocene basalt eruptions in the areas east and west of Cairo, J. Afr. Earth Sci., 21,
455 407-419.

456 Lurcock, P. C. and G. S. Wilson, 2012. PuffinPlot: A versatile, user-friendly program for
457 paleomagnetic analysis, Geochemistry, Geophysics, Geosystems, 13, Q06Z45,
458 doi:10.1029/2012GC004098.

459 Meineissy M.Y., 1990. Vulcanicity in The Geology of Egypt, Said, R. eds, 157-172,
460 Balkema, Rotterdam, Brookfield.

461 Mohamed F.H., 2001. The Natash alkaline volcanic field, Egypt: geochemical and
462 mineralogical inferences on the evolution of a basalt to rhyolite eruptive suite. Journal
463 of Volcanology and Geothermal Research, 105, 291-322.

464 Mostafa R., Khashaba A., El-Hemaly I.A., Takla E.M., Abdel Aal E., and Odah H., 2016.
465 1st paleomagnetic investigation of Nubia Sandstone at Kalabsha, south Western Desert of
466 Egypt. NRIAG J. Geophys., 5, 254-262.

467 Niazi H., and Mostafa M.O., 2002. A paleomagnetic study of the Tertiary basaltic lava flows
468 around Wadi Hudayn Shalatayn area, south Eastern Desert, Egypt. Annals Geol Survey
469 Egypt, 25, 429-442.

470 Odah H., 2004. Paleomagnetism of the Upper Cretaceous Bahariya Formation, Bahariya
471 Oasis, Western Desert, Egypt. J. Appl. Geophys., 3, 2, 177-187.

472 Perrin M., Saleh A., Alva-Valdivia L.M., 2009. Cenozoic and Mesozoic basalts from Egypt: a
473 preliminary survey with a view to paleointensity. Earth Planet. Sc., 61, 51-60.

- 474 Ressetar R., Nairn A.E.M., Monrad J.R., 1981. Two phases of Cretaceous-Tertiary
475 magmatism in the eastern desert of Egypt: paleomagnetic, chemical and K-Ar evidence.
476 *Tectonophysics*, 73, 169-193.
- 477 Reynolds R.L., , 1982. Paleomagnetic research in Egypt. *Report Geol. Surv. Egypt*, 22, 1-12.
- 478 Saradeth S., Soffel H., Schult A., 1987. Palaeomagnetism of sedimentary rocks of the
479 uppermost Cretaceous from the oases of Dakhla and Kharga in the western desert of
480 Egypt. *J. Geophys.*, 61, 64-66.
- 481 Schult A., Hussain A.G., Soffel H.C., 1981. Paleomagnetism of Upper Cretaceous Volcanics
482 and Nubian Sandstones of Wadi Natash, SE Egypt and implications for the Polar
483 Wander Path for Africa in the Mesozoic. *J. Geophys.*, 50, 16-22.
- 484 Schult A., Soffel H.C., Hussain A.G., 1978. Palaeomagnetism of Cretaceous Nubian
485 Sandstone, Egypt. *J. Geophys.*, 44, 333-340.
- 486 Tauxe, L., Kodoma, K.P., Kent, D.V., 2008. Testing corrections for paleomagnetic inclination
487 error in sedimentary rocks: a comparative approach. *Phys. Earth Planet. Inter.*, 169, 152-
488 165.
- 489 Tauxe, L., R. Shaar, L. Jonestrask, N. L. Swanson-Hysell, R. Minnett, A. A. P. Koppers, C.
490 G. Constable, N. Jarboe, K. Gaastra, L. Fairchild, 2016. PmagPy: Software package for
491 paleomagnetic data analysis and a bridge to the Magnetism Information Consortium
492 (MagIC) Database, *Geochem. Geophys. Geosyst.*, 17, 2450– 2463,
493 doi:10.1002/2016GC006307.
- 494 Torsvik, T.H., Muller R.D., Van der Voo, R., Steinberger, B., Gaina, C, 2008. Global Plate
495 Motion Frames: Toward A Unified Model. *Reviews of Geophysics*, 46, RG3004.
- 496 Vahle C., Kontny A., Gunnlaugsson H.P. Kristjánsson L., 2007. The Stardalur magnetic
497 anomaly revisited - new insights into a complex cooling and alteration history. *Phys.*
498 *Earth Planet. Inter.*, 164, 119-141.

499 **TABLE CAPTIONS**

500 Table 1. Mean paleomagnetic results by site and by area. P: Polarity (R/N: Reverse/Normal);
501 D/I: Declination/Inclination; B/N: number of sites/samples; $(\alpha_{95,k})/(A_{95,K})$: Fisher
502 statistic for the direction/pole; °N/°E: Latitude/Longitude; P: polarity
503 (Normal/Reverse).

504 Table 2. Published Cenozoic and Cretaceous paleomagnetic poles for Egypt. °N/°E:
505 Latitude/Longitude; B/N: number of sites/samples; $(A_{95,K})$: Fisher statistic.

506 Table 3. (Supplementary Material) Compilation of all site level paleomagnetic poles obtained
507 from Cenozoic and Cretaceous rocks from Egypt. °N/°E: Latitude/Longitude; N:
508 number of samples; $(A_{95,K})$: Fisher statistic; R: Rocks (I/S/O:
509 Igneous/Sediments/Iron ore).

510 Table 4. Recalculated poles for the Cenozoic and Cretaceous of Egypt. Acc: Acronym; °N/°E:
511 Latitude/Longitude; B: number of sites; $(A_{95,K})$: Fisher statistic.

512

513 **FIGURE CAPTIONS**

514 Figure 1. Cenozoic (circle) and Cretaceous (square) paleomagnetic sites for Egypt.
515 Light/dark: literature/our sites (this study & Perrin et al, 2009), dots: cities.

516 Figure 2. Heating/cooling cycles of representative K–T experiments.

517 Figure 3. Equal-area plot, orthogonal diagram, and demagnetization curve for representative
518 samples: a) 2 components of magnetization; b) single component of magnetization;
519 c) partial IRM remagnetization. Open/full squares: vertical/horizontal projections on
520 the orthogonal plots and negative/positive inclination on the equal area plots.
521 Red/black symbols: selected/not selected demagnetization step.

522 Figure 4. Equal-area plot with ChRM directions per area. Open/full circles: negative/positive
523 inclination.

524 Figure 5. Summary of our paleomagnetic results: a) ChRMs per site, b) ChRMs per area, and
525 c) VGPs compared to BC2002 (red) and T2008 (yellow) MPWPs for South Africa.

526 Figure 6. Paleomagnetic poles published for Egypt (Table 2), compared with the BC2002
527 MPWP: a) without selection; and b) only poles with kappa larger than 50. Blue/red:
528 Cenozoic /Cretaceous poles. Light/dark: literature/our sites (this study & Perrin et al,
529 2009).

530 Figure 7. Cenozoic poles at the site level for Egypt: a) temporal distribution, b) all site poles,
531 c) Shalaten poles, d) selected poles ($\kappa > 50$), e) recalculated poles (Table 4), new
532 Cenozoic path for Egypt (dashed arrow) and BC2002 MPWP (full line). Dark/Light
533 A_{95} circles: Igneous/sediments.

534 Figure 8. Cretaceous poles at the site level for Egypt: a) all site poles, b) selected poles
535 ($\kappa > 50$), c) recalculated poles (Table 4) compared to BC2002 MPWP (full grey
536 line). Dark/Light A_{95} circles: Igneous/sediments.

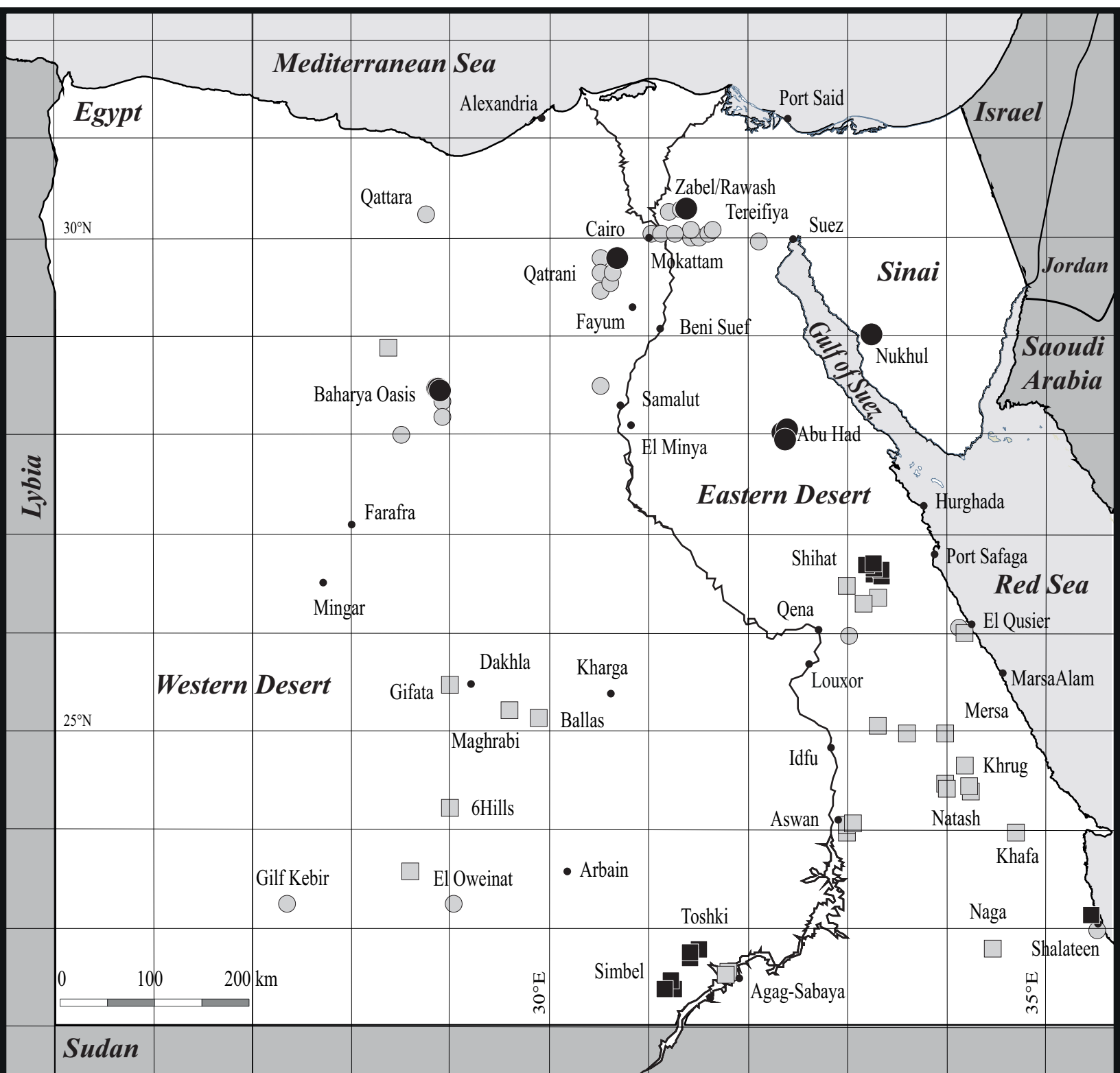


Figure 1

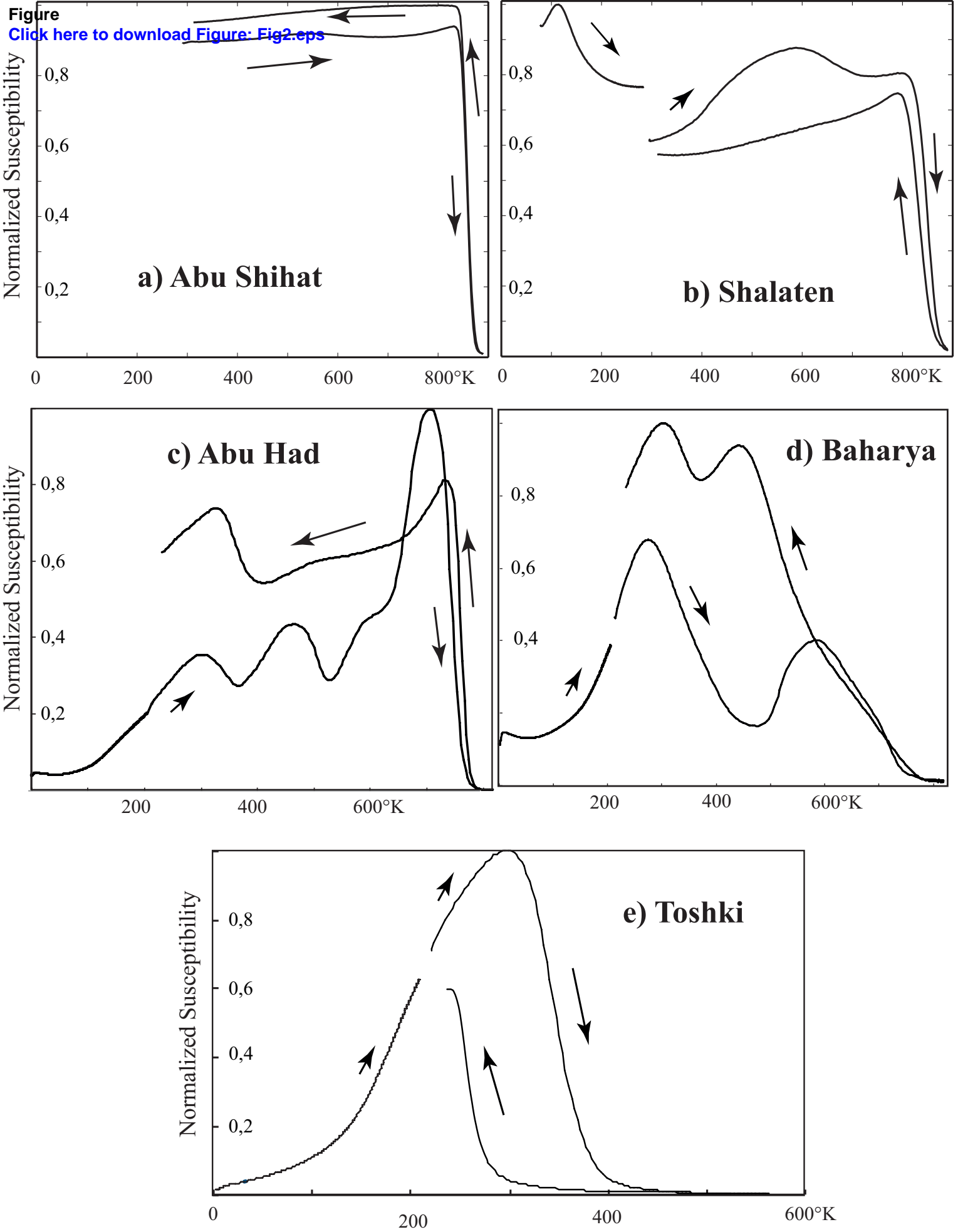
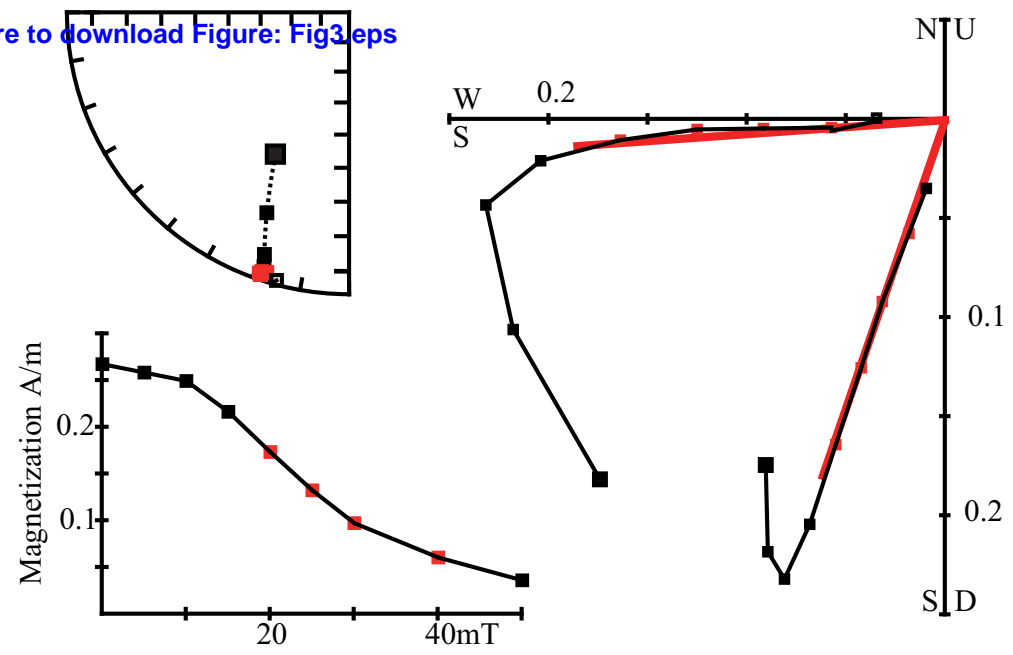


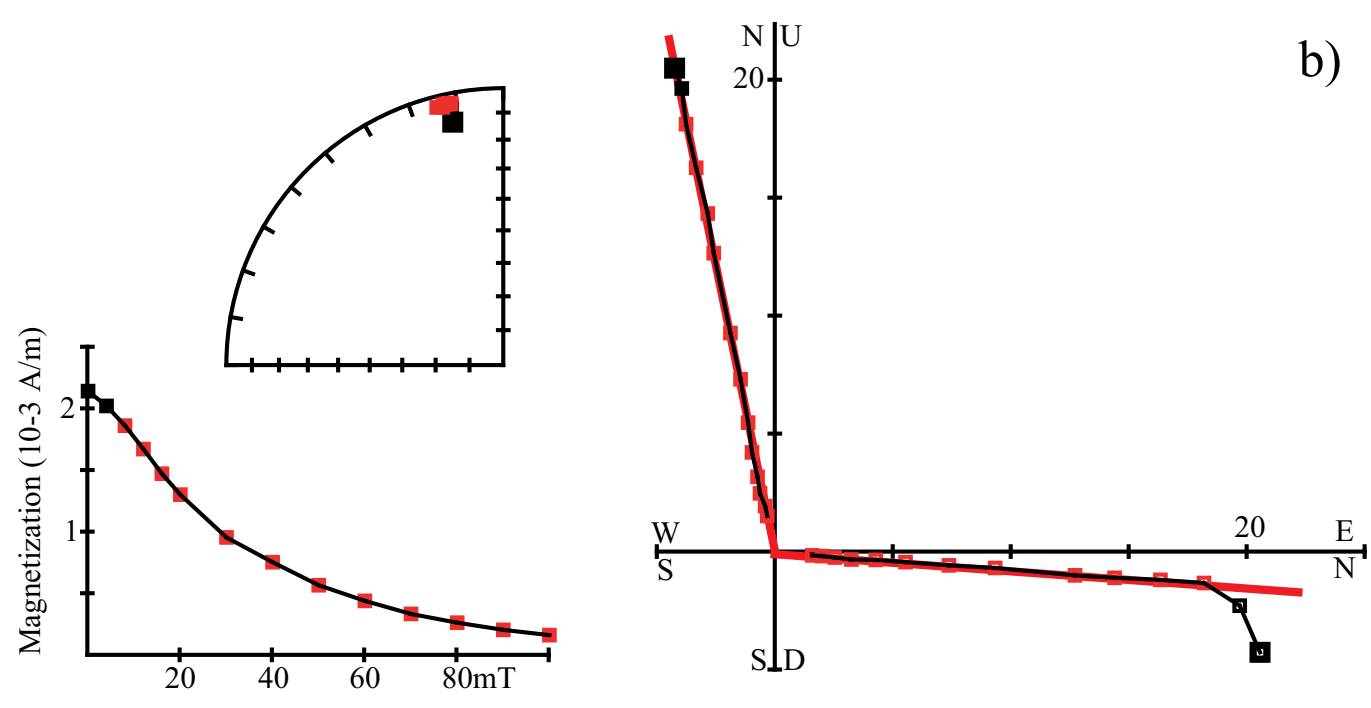
Figure 2

Figure
[Click here to download Figure: Fig3eps](#)

a)



b)



c)

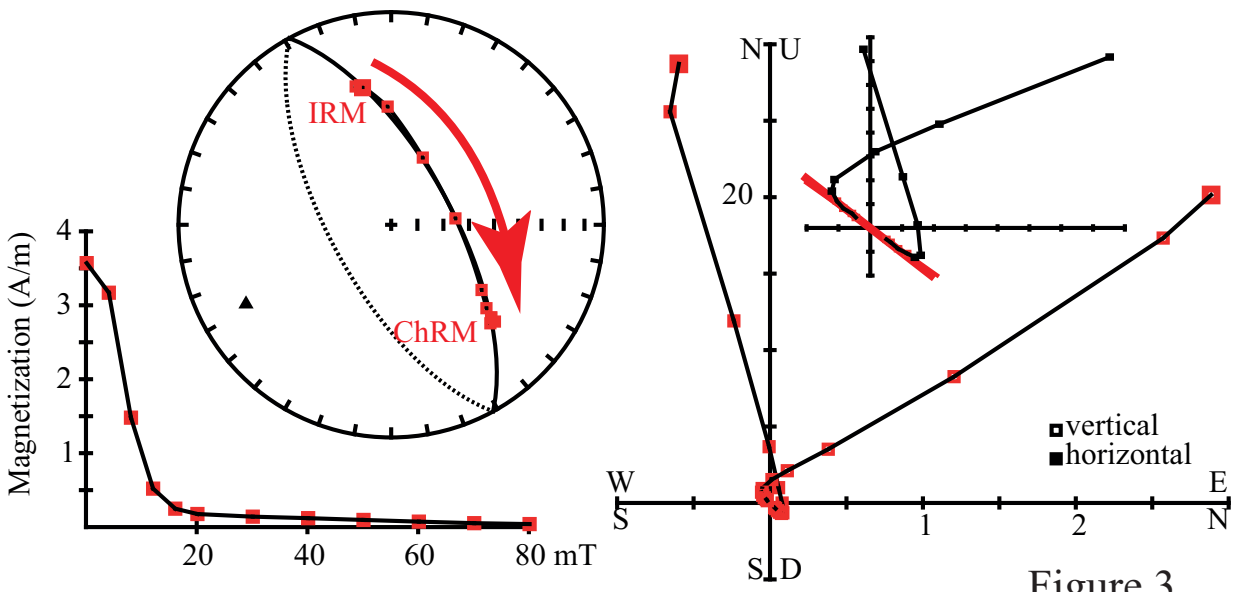


Figure 3

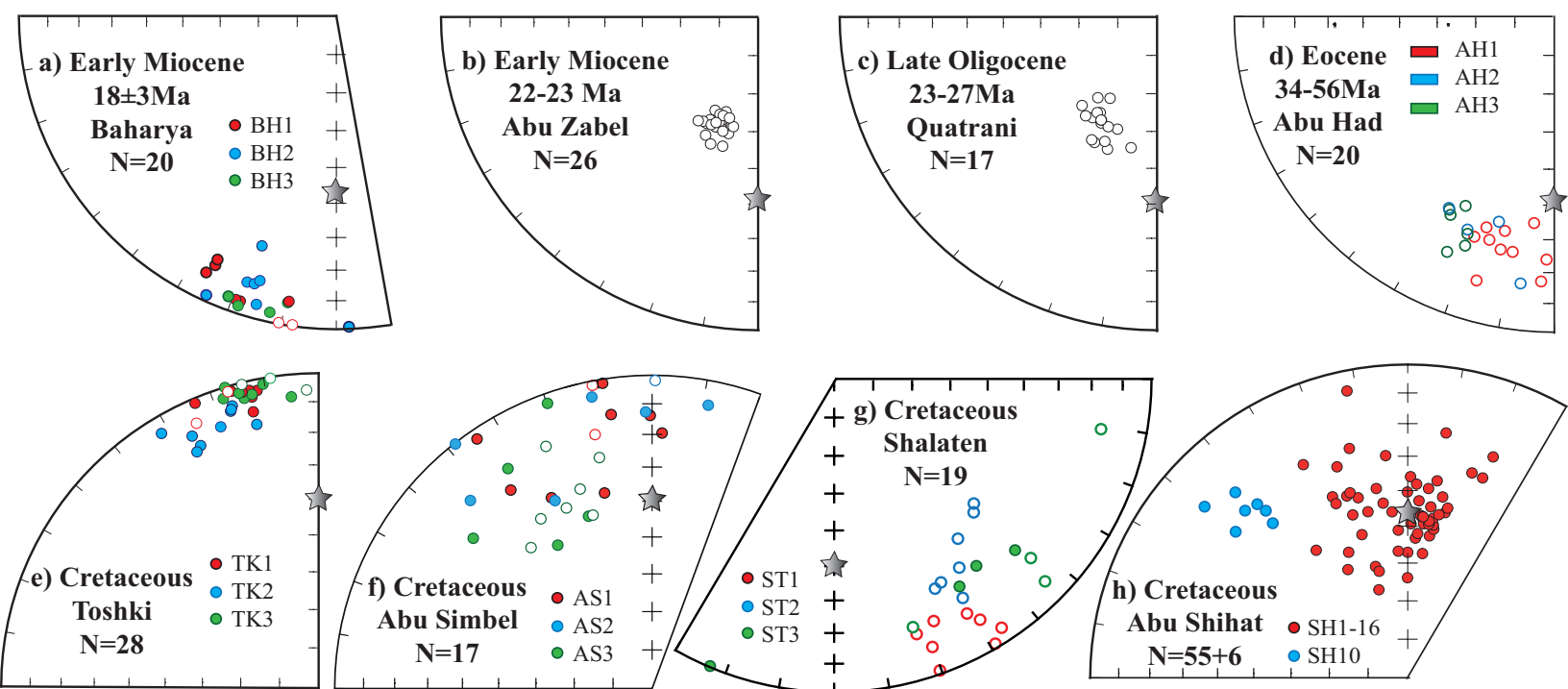


Figure 4

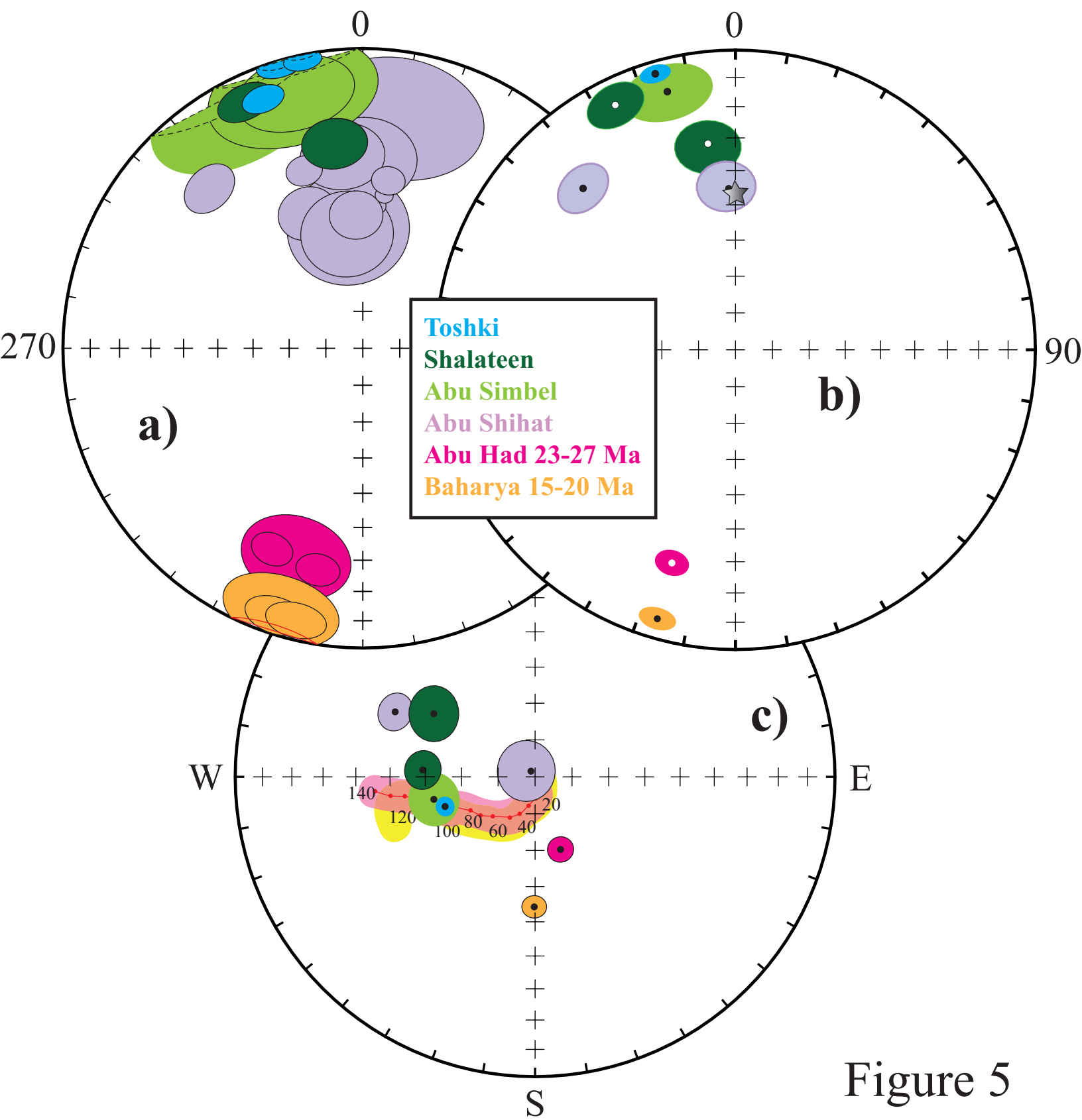


Figure 5

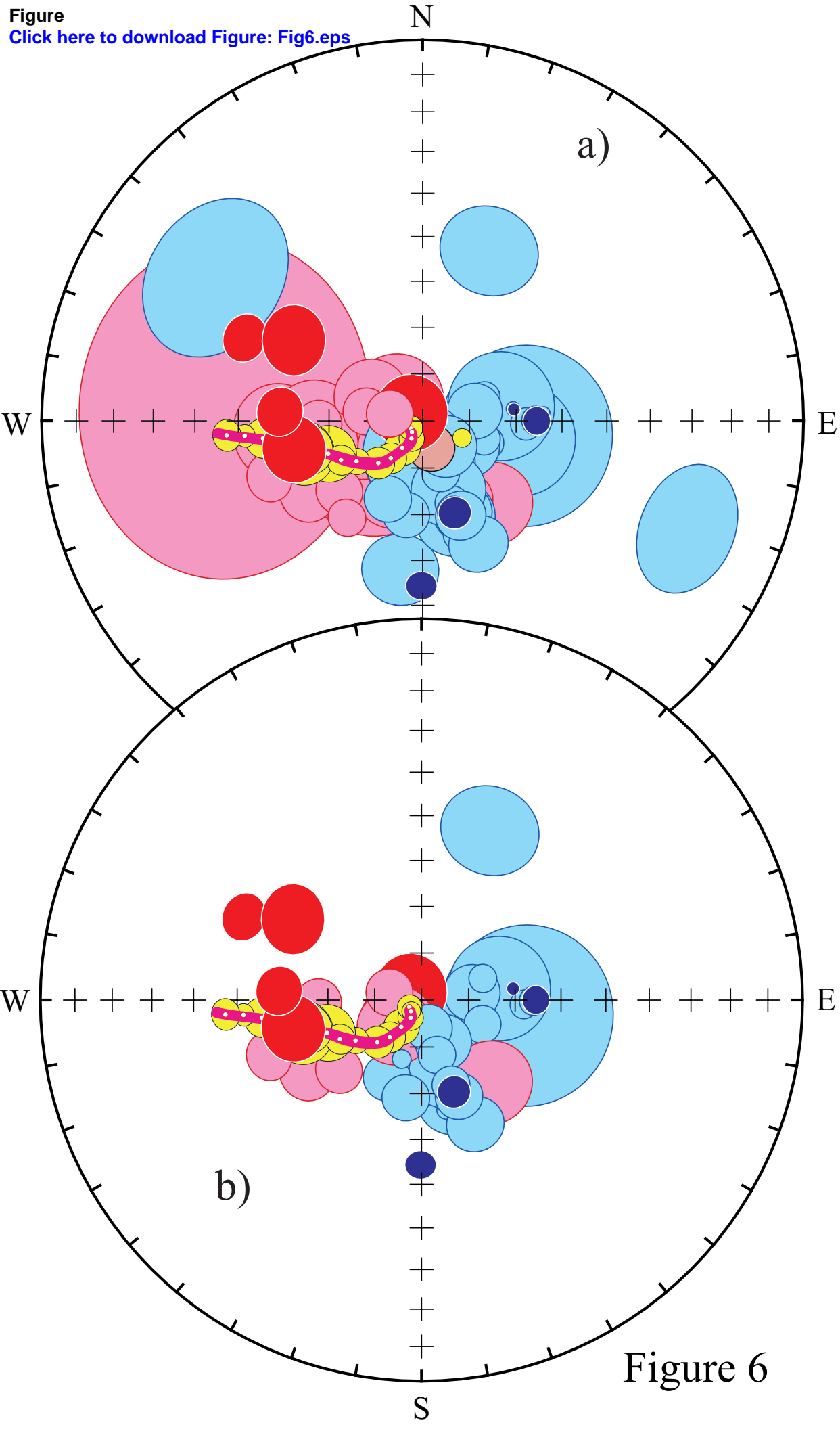
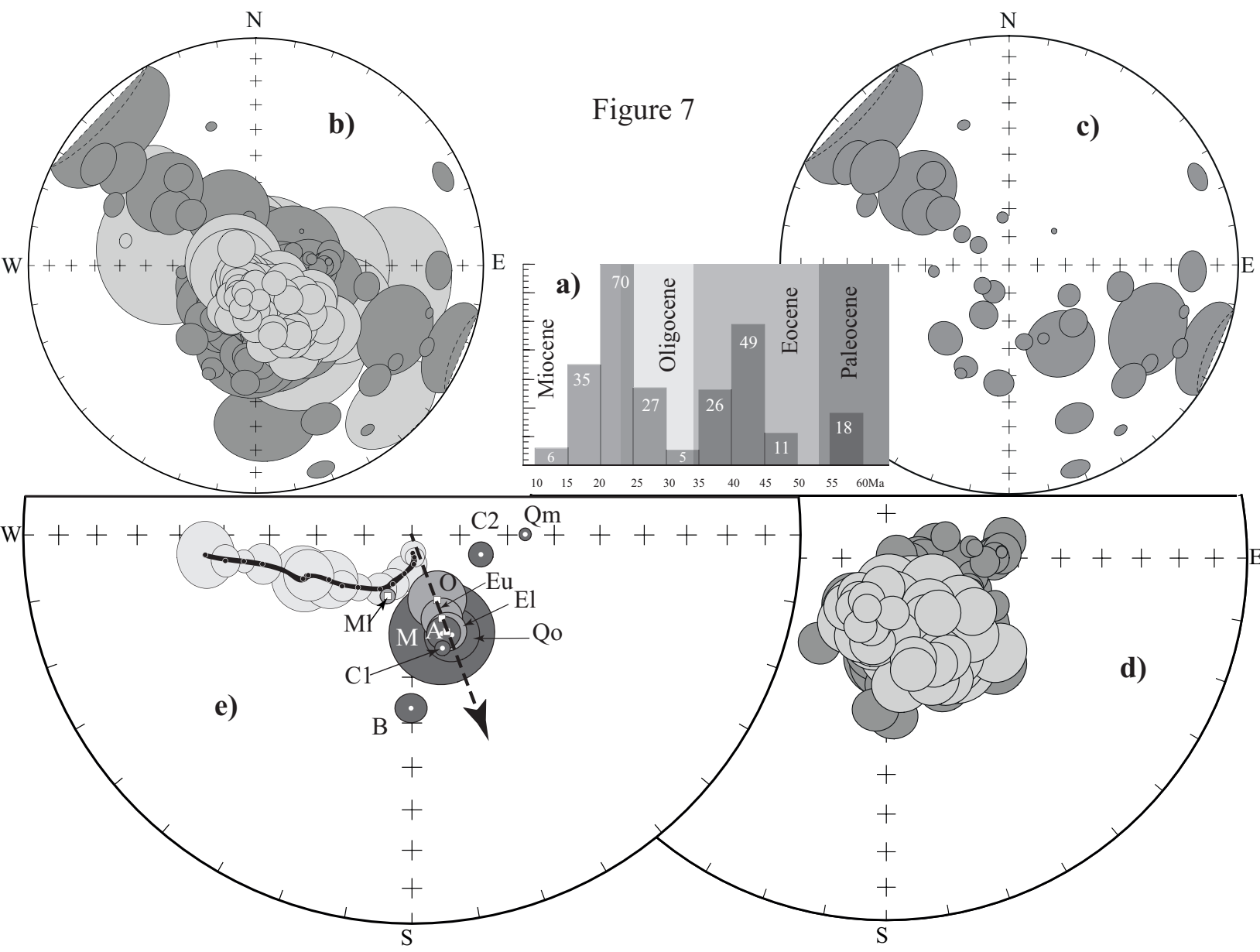
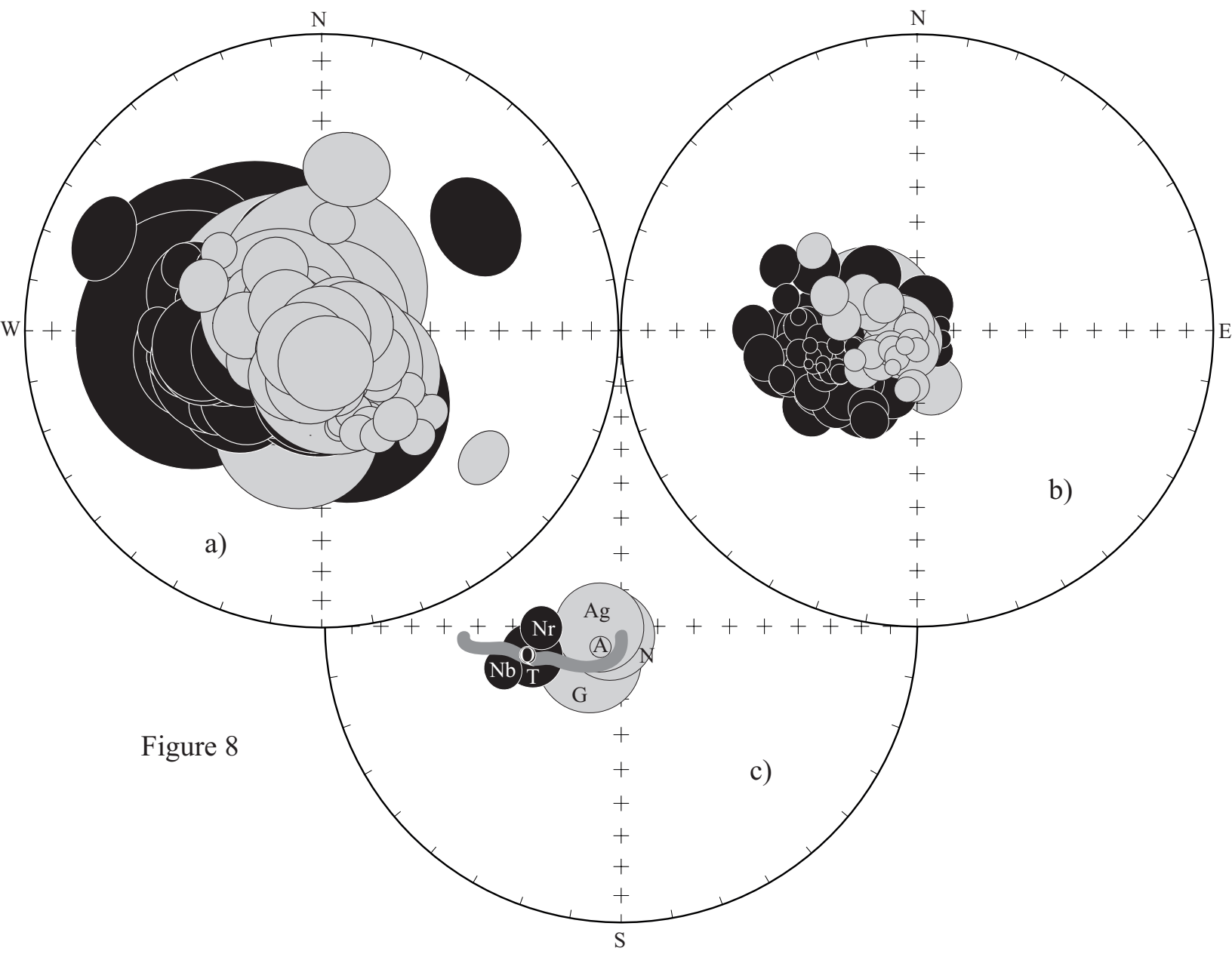


Figure 6





[Click here to download Table: Table1.xlsx](#)

Area	P	Mean direction						Pole				
		Site	B	N	D	I	α_{95}	k	$^{\circ}E$	$^{\circ}N$	A_{95}	K
Baharya	R	BH1	8	198	7	6.6	72					
		BH2	8	194	7	6.3	78					
		BH3	4	197	9		57					
		BH	20	196	7	3.8	75	180	54	3.2	108	
		3	196	8		1101						
Abu Had	R	AH1	10	192	-26	5.1	92					
		AH2	4	198	-27		51					
		AH4	6	204	-28	5.0	179					
		AH	20	197	-27	3.9	72	161	69	3.5	86	
		3	198	-27		192						
Shalaten	R	ST1	8	335	10	6.1	83	273	59	4.9	131	
		ST2	7	352	32	7.8	61	302	57	7.2	72	
Toshki	N	TK1	9	344	2	4.7	123					
		TK2	9	338	11	4.6	125					
		TK3	10	348	2	3.8	159					
		TK	28	344	5	3.1	79	252	64	2.5	122	
		3	343	5		119						
Abu Simbel	N	AS1	10	345	13	###	15					
		AS2	7	345	12	###	12					
		AS3	12	333	-9	###	6					
		AS	29	340	4	###	8	258	62	7.0	16	
Abu Shihat	N	SH1	4	354	35		82					
		SH2	5	338	50	7.6	102					
		SH4	4	352	58		59					
		SH5	5	342	37	4.5	294					
		SH8	6	6	50	2.4	762					
		SH9	6	357	53	6.9	94					
		SH11	6	8	47	2.3	845					
		SH12	6	9	43	4.2	259					
		SH13	6	0	37	###	28					
		SH15	3	353	57		61					
		SH16	4	8	22		22					
		SH	55	358	45	3.5	31					
			11	357	45	7.5	38	323	87	7.2	41	
SH10	6	316	27	6.6	105	295	48	4.9	186			

[Click here to download Table: Table2.xlsx](#)

Reference	Site		Age		B	N	Pole				
	Locality	°N	°E	Ma ±			°N	°E	Age K		
El-Shazly, Krs, 1973	Aswan	###	###	88	8	5	12	75	203	9	34
El-Shazly, Krs, 1973	Natash	###	###	88	8	9	##	64	218	4	8
Hussain et al, 1976a	Zabel	###	###	23	1	1	17	76	70	3	##
Hussain et al, 1976a	Rawash	###	###	28	5	1	17	79	81	6	##
Hussain et al, 1976b	Aswan	###	###	83	#	9		81	200	9	37
Hussain et al, 1976b	Safaga	###	###	83	#	10		83	311	10	26
Hussain, 1977	Baharya	###	###	44	#	7		84	163	5	##
Schult et al, 1978	Aswan	###	###	83	#	18	##	80	227	5	47
Hussain et al, 1979	Mandisha	###	###	17	#	2	30	58	187	8	
Hussain et al, 1979	Tereifiya	###	###	44	4	6	##	69	189	5	##
Hussain et al, 1979	Shihat	###	###	##	#	4	30	45	273	34	
Hussain et al, 1980	Qatrani	###	###	25	2	15	41	64	87	1	##
Ressetar et al, 1981	Egypt	###	###	20	#	7	60	68	102	12	27
Ressetar et al, 1981	Qusier	###	###	81	#	16	92	63	252	2	##
Ressetar et al, 1981	Natash	###	###	83	5	5	24	76	228	15	26
Ressetar et al, 1981	Khafa	###	###	88	6	4	18	61	238	6	##
Ressetar et al, 1981	Khrug	###	###	89	0	6	16	59	266	10	44
Schult et al, 1981	Qatrani	###	###	26	4	3		73	81	11	##
Schult et al, 1981	Natash	###	###	93	7	15	##	69	258	7	31
Schult et al, 1981	Baharya	###	###	36	2	9		84	139	7	60
Schult et al, 1981	Natash	###	###	93	7	5	##	83	231	8	94
Reynolds, 1982	Zabel	###	###	23	1	1	5	68	92	3	##
Hussain, Aziz, 1983	Oweinat	###	###	34	#	5	##	74	160	8	64
Hussain, Aziz, 1983	Oweinat	###	###	83	#	10	##	68	269	10	19
Hussain, Aziz, 1983	Oweinat	###	###	83	#	7	82	77	258	9	49
Saradeth, 1987	Gifata	###	###	68	3	7	##	82	225	8	60
Lofty, 1995	Cairo	###	###	18	0	16	##	76	111	4	##
Lofty, 1995	Cairo	###	###	23	0	11	##	66	167	2	##
Abdeldayem, 1996	Qattara	###	###	14	9	11	64	77	198	2	##
Lofty, Odah, 1998	Cairo	###	###	21	7	66		76	107	3	27
Lofty, Odah, 1998	Cairo	###	###	23		43		66	164	4	31
Lofty, Odah, 1998	Cairo	###	###	20	3	27		79	119	7	18
Lofty, Odah, 1998	Cairo	###	###	36	2	58		64	162	3	26
Abdeldayem, 1999	Qatrani	###	###	24	0	2	15	67	98	19	##
Abdeldayem, 1999	Qatrani	###	###	25	2	9	64	80	151	6	74
Abdeldayem, 1999	Mokattam	###	###	45	#	11	91	78	163	4	##
Niazi, Mostafa, 2002	Shalatayn	###	###	34	#	16	84	83	190	11	12
Niazi, Mostafa, 2002	Shalatayn	###	###	34	#	4	22	50	22	10	84
Niazi, Mostafa, 2002	Shalatayn	###	###	34	#	5	33	34	305	16	25
Niazi, Mostafa, 2002	Shalatayn	###	###	34	#	8	43	25	112	12	23
Kent, Dupuis, 2003	Safaga	###	###	50	#	2	71	88	159	3	45
Lofty, Abd El-All, 200	Bahnasa	###	###	26	3	5	31	68	161	8	85
Lofty, Abd El-All, 200	Minia	###	###	43	5	9	51	61	156	6	71
Abd El-All, 2004	Naga	###	###	##	#	14	##	68	268	5	64
Odah, 2004	Baharya	###	###	95	5	14	70	71	151	6	
Lotfy, VanderVoo, 200	Qatrani	###	###	29	6	13	87	68	158	6	49
Lotfy, VanderVoo, 200	Qatrani	###	###	42	8	38	##	70	159	4	55
Perrin et al, 2009	Zabel	###	###	23	1	2	26	70	83	1	##
Perrin et al, 2009	Qatrani	###	###	25	2	2	17	66	90	3	##
Lofty, 2011	Natash	###	###	82	4	10	61	67	229	5	96
Lofty, 2011	Natash	###	###	##	7	12	68	55	250	5	84
Lofty, 2011	Natash	###	###	92	2	8	44	86	223	9	41
El-Shayeb et al, 2013	Maghrabi	###	###	83	#	5	38	66	141	9	78
El-Shayeb et al, 2013	6Hill/Bak	###	###	##	#	11	96	78	294	8	
Lofty, Odah, 2015	Gilf Kebir	###	###	59	2	13	84	72	204	5	73
Mostafa et al, 2016	Aggag	###	###	83	#	4	57	83	283	5	51
Mostafa et al, 2016	Sabaya	###	###	83	#	5	75	78	280	5	21

[Click here to download Table: Table4.xlsx](#)

Site		Age			Pole				
Name	Acc	Ma	±	B	°E	°N	A ₉₅	K	
Baharya igneous	B	18	3	3	180	54	3.2	108	
Cairo igneous	C1	21	2	11	164	66	1.6	815	
Cairo igneous	C2	23	5	23	103	75	2.6	140	
Qatrani igneous	Qm	23	3	7	88	66	1.3	2035	
Minia igneous	Mi	26	3	4	162	69	10.9	72	
Qatrani igneous	Qo	29	6	13	157	68	5.7	53	
Abu Had igneous	A	45	11	3	161	69	3.5	86	
Qatara sediments	Qa	18	6	9	202	77	1.6	983	
Qatrani sediments	Q	37	8	41	158	71	3.0	55	
Minia sediments	Mi	43	5	5	159	60	8.4	84	
Mokatam sediments	Mo	45	11	7	162	77	6.2	96	
Qusier basalt	Q	81	13	16	253	63	2.3	266	
Natash basalt	Nb	104	7	12	250	55	5.4	66	
Naga ring complex	Nr	140	15	12	269	68	5.9	55	
Toshki basalt	T	106	40	3	252	64	8.7	201	
Natash sediments	N	92	2	4	231	86	12.3	57	
Aswan sediments	A	83	17	8	225	82	2.9	365	
Agag sediments	Ag	92	2	3	267	84	12.2	103	
Gifata sediments	G	74	4	3	223	77	14.3	75	